Structural and superconducting transition in selenium at high pressure

doi: 10.1103/PhysRevB.63.104516

Structural and superconducting transition in selenium at high pressure

M. Otani*
Division of Material Physics, Department of Physical Science, Graduate School of Engineering Science, Osaka University, 1-3 Machikaneyama-cho, Toyonaka 560–8531, Japan

N. Suzuki
Division of Material Physics, Department of Physical Science, Graduate School of Engineering Science, Osaka University, 1-3 Machikaneyama-cho, Toyonaka 560–8531, Japan
and ''Research Area'' CREST, Japan Science and Technology Corporation, Japan

(Received 27 April 2000; revised manuscript received 29 September 2000; published 20 February 2001)

First-principles calculations are performed for electronic structures of two high-pressure phases of solid selenium, β-Po, and bcc. Our calculation reproduces well the pressure-induced phase transition from β-Po to bcc observed in selenium. The calculated transition pressure is 30 GPa lower than the observed one, but the calculated pressure dependence of the lattice parameters agrees fairly well with the observations in a wide range of pressure. We estimate the superconducting transition temperature T_c of both the β-Po and the bcc phases by calculating the phonon dispersion and the electron-phonon interaction on the basis of density-functional perturbation theory. The calculated T_c shows a characteristic pressure dependence. In bcc Se, T_c increases considerably with decreasing pressure and its maximum may exceed 10 K. In β-Po Se, T_c depends sensitively on the lattice constants we have used. For the lattice constants estimated by calculation, the values of T_c is as high as that in bcc phase and decreases with increasing pressure. For the lattice constants determined by measurements, on the other hand, T_c is less pressure dependent and there is a large jump in T_c at the transition from β-Po to bcc.

DOI: 10.1103/PhysRevB.63.104516 PACS number(s): 74.25.Kc, 61.50.Ks, 71.15.Mb, 74.25.Jb

I. INTRODUCTION

Recently, with the development of high-pressure experimental techniques, research on pressure-induced structural phase transitions of the group VIb elements O, S, Se, and Te has progressed greatly. At high-pressures both metallic tellurium (Te) and selenium (Se) transform from β-Po to bcc phase at 27 GPa (Ref. 1) and 150 GPa,[2] respectively. The β-Po type structure is rhombohedral and can be described as a simple cubic lattice deformed along the [111] direction keeping the edge length unchanged. By changing the ratio c/a of the rhombohedral lattice we obtain the bcc structure when $c/a=\sqrt{6}/4$. In Te superconducting transitions are observed in both β-Po and bcc structures at low temperature and a jump in T_c from 2.5 to 7.4 K is observed at 32–35 GPa.[2] Theoretically, Mauri, *et al*. suggests that the jump in T_c is related to the phonon softening in the bcc phase, namely with decreasing pressure the phonon anomaly enhances the electron-phonon coupling.[3] In Se, on the other hand, there is neither experimental observation nor *ab initio* calculation for the pressure dependence of phonon frequencies, the electron-phonon interaction or T_c.

The purpose of the present paper is to estimate these quantities by using *ab initio* calculations. First we calculate the total energies of the β-Po and bcc phases of Se by using the full-potential linearized muffin-tin orbital (FPLMTO) method[4] in order to discuss the pressure-induced phase transition from β-Po to bcc. Then we calculate phonon frequencies and electron-phonon coupling constants using the linear-response FPLMTO (LR-FPLMTO) method.[5,6] The validity of this method is demonstrated in Refs. 5–8. Finally we calculate the superconducting transition temperature in both the β-Po and bcc phases as a function of pressure.

II. STRUCTRAL TRANSITION FROM β-Po TO BCC IN SELENIUM

A. Calculational procedure

The calculations of electronic states for the β-Po and bcc structures of Se have been done according to the following procedure with use of the FPLMTO program. For exchange-correlation functional we have adopted the formula proposed by Gunnarsson and Lundqvist[9] and the generalized gradient approximation (GGA) correction proposed by Perdew *et al.*[10] has been taken into account. Inside the muffin-tin (MT) spheres the scalar-relativistic calculations are performed for valence electrons, and the core states are recalculated at each self-consistent iteration with relativistic effects. The MT radius has been taken to be 1.07 Å. The $\boldsymbol{k}$-space integration has been performed by the improved tetrahedron method[11] with use of (12, 12, 12) grid of the sampling $\boldsymbol{k}$ points [189 points in the irreducible Brillouin zone (IBZ)]. We have used 3κ-spd-LMTO basis set (27 orbitals): $\kappa^2=-0.1$, -1.0, and -2.0 Ryd. In the interstitial region the basis functions are expanded in plane waves up to the cutoff corresponding approximately to 200, 350, and 650 plane waves per *s*, *p*, and *d* orbitals, respectively. The charge densities and the potentials are expanded inside the MT spheres by spherical harmonics up to $l_{max}=6$ and in the interstitial region by plane waves with the cutoff corresponding to the (16, 16, 16) fast-Fourier-transform (FFT) grid in the unit cell of direct space. The final convergence is within 10^{-6} Ryd.

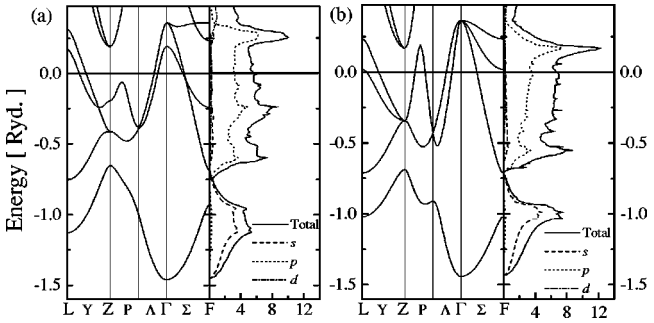

FIG. 1. The band structure and the density of states of Se at atomic volume $V=14.82$ Å: (a) β-Po type structure and (b) bcc structure. The horizontal line denotes the Fermi level.

B. Results

As the first step to investigate the phase transition from β-Po to bcc we have calculated the electronic band structure and the total energy of β-Po Se at atomic volume $V_A = 14.82$ Å. At this volume the β-Po structure is known to be stable by experimental measurements. For comparison we have calculated the electronic band structure and the total energy of the hypothetical bcc structure with the same atomic volume. The calculated energy band structures and the density of states (DOS) for the β-Po and the bcc structures are shown in Fig. 1. The lowest band is mainly derived from the $4s$ component and the next three bands from the $4p$ component. The band structures of both the structures are similar to each other on the whole. However, remarkable differences can be seen in the band structure and the DOS near the Fermi level. Firstly, the band structure of the bcc structure along the P and Λ lines has much larger dispersion than that of the β-Po-type structure. Secondly, the DOS at the Fermi level of the bcc structure is larger than that of the β-Po structure because in bcc Se the L point is a saddle point of the third energy band from the bottom which crosses the Fermi level near the L point. By deforming from bcc to β-Po the L point energy of the third band goes up away from the Fermi level and the states of the fourth band in the middle of the P line come down under the Fermi level. As a result the DOS of β-Po Se has a relatively large peak at 0.225 Ryd. below the Fermi level. This is the reason why the β-Po-type structure is relatively more stable compared with the bcc structure.

To investigate the pressure-induced structural transition we have to calculate the total energy of the β-Po and the bcc structures as a function of volume. For the β-Po structure we have optimized c/a at each volume, namely, we have calculated the total energy of the β-Po type Se as a function of c/a with the atomic volume V_A being kept constant. Figure 2 shows the total energy vs c/a for several fixed atomic volume and the inset shows the results for a volume range near the phase transition. All the energies are referenced to that of the bcc structure, i.e., the energy at $c/a=\sqrt{6}/4$. For a large volume such as 16.30 Å^3 the energy takes the minimum at $c/a \sim 0.85$ and the c/a of bcc is an inflection point. With decreasing volume the value of the c/a starts to decrease gradually toward the bcc structure. Finally, the β-Po structure is no longer a quasistable structure, that is, the total energy has a single minimum at $c/a=\sqrt{6}/4$ corresponding to the bcc structure.

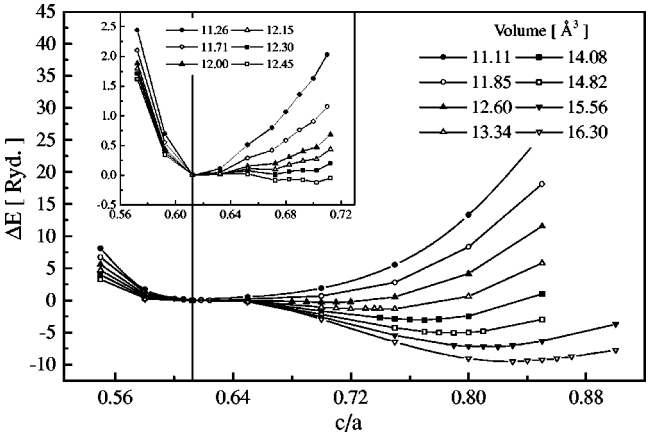

FIG. 2. The total energy of β-Po Se as a function of c/a for the fixed atomic volume. The inset indicate the results for volumes near the phase transition. All the energies are referenced to the bcc structure, i.e., $\Delta E = E - E_{bcc}$.

Figure 3 shows the total energy of the β-Po and the bcc structures of Se as a function of volume. At larger volumes the β-Po structure is more stable than the bcc structure. At smaller volumes the total energies of both the structures are quite close, but the bcc structure is more stable than the β-Po structure at volumes smaller than ~ 12 Å^3.

It is noted here that the transition from β-Po to bcc is nearly second-order character and hence it is rather difficult to see clearly the crossing behavior of the two energy curves even in enlarged energy scale. If we plot the Gibbs free energy defined in the following, however, we can clearly recognize the crossing of the two free-energy curves as a function of pressure (see the inset of Fig. 3).

In order to estimate the transition pressure from β-Po to bcc we calculate the Gibbs free energy (or enthalpy) as a function of pressure. Then, to evaluate the pressure as a func-

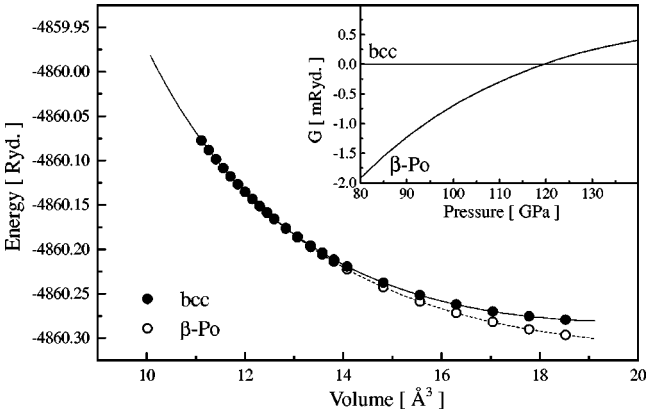

FIG. 3. The total energy calculated as a function of volume for the β-Po and the bcc structures of Se. The lines are obtained by using Murnanghan's equation of state. The inset depicts the Gibbs free energies (G) as a function pressure near the phase transition. The free energy of the bcc phase is taken to be the origin of G.

tion of volume we fitted the calculated total energies by the Murnaghan's equation of state (EOS):[12]

$$E(V)=\frac{B_0V}{B_0'}\left[\frac{1}{B_0'-1}\left(\frac{V_0}{V}\right)^{B_0'}+1\right]+\text{const},$$

where B_0 and B_0' is the isothermal bulk modulus at zero pressure and it's derivative, respectively. The pressure is determined from

$$P=\frac{B_0}{B_0'}\left[\left(\frac{V}{V_0}\right)^{-B_0'}-1\right].$$

The Gibbs free energy is defined by $G(P)\equiv E_{\text{tot}}(P)+PV(P)$ and the transition pressure between the two phases is obtained from the relation $G_\beta(P)=G_{\text{b}}(P)$, where G_β and G_{b} are the Gibbs free energies of the β-Po and the bcc structures, respectively.

The transition pressure P_{c} from β-Po to bcc has been estimated as 120 GPa by our present calculation. This value is higher than other calculated transition pressures, 95 GPa (FLAPW method without GGA)[14] and 110 GPa (Pseudopotential method without GGA),[15] but still lower than the experimental value of 150 GPa.[13] The origin of this discrepancy between theory and experiment may be ascribed to the local density approximation (LDA) with GGA itself and/or numerical accuracy of the total energy. With respect to the latter point we note that Fig. 3 shows that the volume-energy curves for the two structures are almost parallel near the phase transition. Therefore a small change in the total energy for one of the phases is expected to cause a large change for the value of P_{c}; if the total energy of one of the two phases is shifted by 1 mRyd., the value of P_c changes by 20 GPa.

Figure 4 shows the pressure dependencies of the atomic volume V_{A}, the lattice constants a and c, and the bond lengths r_1 and r_2 which are defined as the nearest neighbor (n.n.) and next n.n.(n.n.n) atomic distances, respectively. Note that in the bcc phase $c=(\sqrt{6}/4)a$, and $r_1=r_2=(\sqrt{3}/2)a$. The filled circles and filled triangles indicate the results of the present calculations and the open squares and open inverse triangles represent the experimental values.[13] The solid and the dashed vertical lines indicate the boundary of the phase transitions determined theoretically by us and experimentally by Akahama *et al.*,[13] respectively.

As seen from Fig. 4 the volume variation as a function of pressure below 120 GPa (β-Po) and above 150 GPa (bcc) shows good agreement with the observations.[13] The obtained pressure dependence of a, c, and the bond lengths of the β-Po phase agree well with the experimental results.[13] Furthermore, the volume reduction at the transition from β-Po to bcc is estimated to be 0.06 Å^3, which is in good agreement with the experimental volume (about 0.08 Å^3).[13]

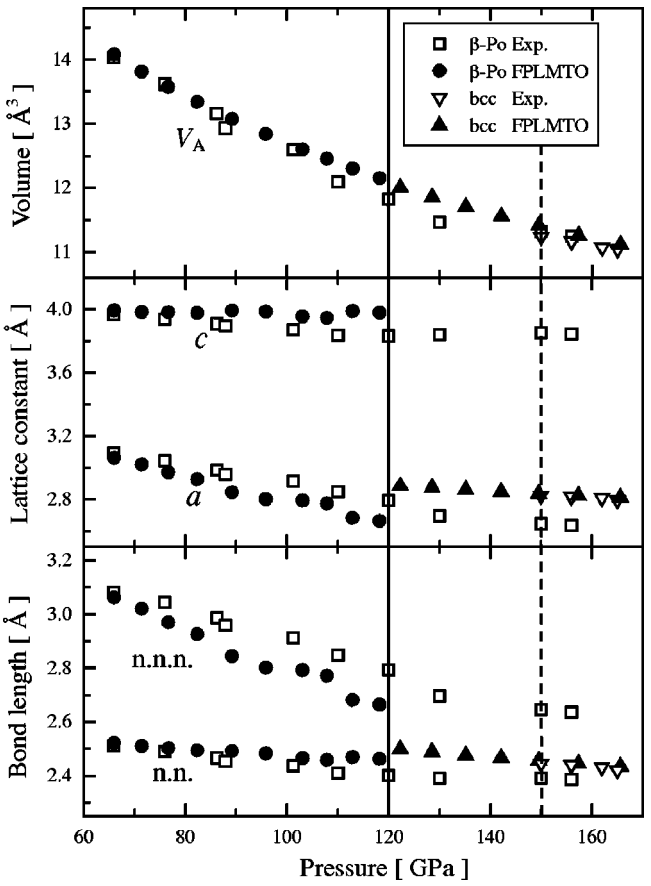

FIG. 4. The pressure dependence of atomic volume, lattice constants, and bond length of selenium. The filled circles and filled triangles indicate the results of the present calculations and the open squares and open inverse triangles represent the experimental values (Ref. 13) The solid and the dashed vertical lines indicate the boundary of the phase transition from β-Po to bcc, determined theoretically by us and experimentally by Akahama *et al.*, respectively.

III. LATTICE DYNAMICS, ELECTRON-PHONON INTERACTION, AND SUPERCONDUCTIVITY

A. Calculational procedure

Actual calculational procedures are as follows. We find the dynamical matrix as a function of wave vector for a set of irreducible $\boldsymbol{q}$ points on a (8, 8, 8) reciprocal lattice grid [29 points in the IBZ] for the bcc structure and (6, 6, 6) reciprocal lattice grid [32 points in the IBZ] for the β-Po structure. The (I,J,K) reciprocal lattice grid is defined in a usual manner: $\boldsymbol{q}_{ijk}=(i/I)\boldsymbol{G}_1+(j/J)\boldsymbol{G}_2+(k/K)\boldsymbol{G}_3$, where $\boldsymbol{G}_1,\boldsymbol{G}_2,\boldsymbol{G}_3$ are the primitive translations in the reciprocal space.

The self-consistent calculations are performed for every wave vector with use of the following basis set and criteria. We use 3κ-spd-LMTO basis set (27 orbitals) with the one-center expansions performed inside the MT spheres up to $l_{max}=6$. In the interstitial region the basis functions are expanded in plane waves up to the cutoff corresponding to 134 (110), 176 (170), and 320 (320) plane waves per *s*, *p*, and *d* orbitals for bcc (β-Po) structure, respectively. The induced charge densities and the screened potentials are represented inside the MT spheres by spherical harmonics up to $l_{max}=6$ and in the interstitial region by plane waves with the cutoff corresponding to the (16, 16, 16) fast-Fourier-transform grid in the unit cell of direct space. The $\boldsymbol{k}$-space integration needed for constructing the induced charge density and the dynamical matrix is performed over the (16, 16,

16) grid [145 points in the IBZ] for the bcc structure and (12, 12, 12) grid [185 points in the IBZ] for the β-Po structure, which is twice denser than the grid of the phonon wave vectors $\boldsymbol{q}$. The integration is performed also by the improved tetrahedron method. However, the integration weights for the $\boldsymbol{k}$ points at these grid have been found to take precisely into account the effects arising from the Fermi surface and the energy bands. This is done with help of the band energies generated by the original FPLMTO method at the (32, 32, 32) grid [897 points in the IBZ] for the bcc structure and (24, 24, 24) grid [1313 points in the IBZ] for the β-Po structure. This procedure allows us to obtain better convergence results with respect to the number of $\boldsymbol{k}$ points.

For calculation of the electron-phonon coupling the corresponding $\boldsymbol{k}$-space integrations are more sensitive than the dynamical matrices to the number of sampling $\boldsymbol{k}$ points. It has been performed with the help of the (32, 32, 32) grid for bcc and (24, 24, 24) for β-Po in the IBZ by means of the tetrahedron method.

The superconducting transition temperature T_c is calculated by using Allen-Dynes formula which is derived on the basis of the strong coupling theory of phonon mechanism. Instead of describing the details of the strong coupling theory, here we give only the necessary equations to calculate T_c. In the following we completely obey the description of the reference.[6]

For the electron-phonon spectral distribution functions $\alpha^2F(\omega)$, we employ the expression[16] in terms of the phonon linewidths $\gamma_{\boldsymbol{q}\nu}$

$$\alpha^2F(\omega)=\frac{1}{2\pi N(\varepsilon_F)}\sum_{\boldsymbol{q}\nu}\frac{\gamma_{\boldsymbol{q}\nu}}{\omega_{\boldsymbol{q}\nu}}\delta(\omega-\omega_{\boldsymbol{q}\nu}), \tag{1}$$

where $N(\varepsilon_F)$ is the electronic density of states per atom and per spin at the Fermi level. When the energy bands around the Fermi level are linear in the range of phonon energies, the linewidth is given by the Fermi ''golden rule'' and is written as follows:

$$\gamma_{\boldsymbol{q}\nu}=2\pi\omega_{\boldsymbol{q}\nu}\sum_{\boldsymbol{k}jj'}|g^{\boldsymbol{q}\nu}_{\boldsymbol{k}+\boldsymbol{q}j',\boldsymbol{k}j}|^2\delta(\varepsilon_{\boldsymbol{k}j}-\varepsilon_F)\delta(\varepsilon_{\boldsymbol{k}+\boldsymbol{q}j'}-\varepsilon_F), \tag{2}$$

where $g^{\boldsymbol{q}\nu}_{\boldsymbol{k}+\boldsymbol{q}j',\boldsymbol{k}j}$ is the electron-phonon matrix element, and conventionally written in the form

$$g^{\boldsymbol{q}\nu}_{\boldsymbol{k}+\boldsymbol{q}j',\boldsymbol{k}j}=\langle\boldsymbol{k}+\boldsymbol{q}j'|\,\delta^{\boldsymbol{q}\nu}V_{\rm eff}|\boldsymbol{k}j\rangle, \tag{3}$$

where $\boldsymbol{k}j$ denotes the one-electron basis $\Psi_{\boldsymbol{k}j}$ and $\delta^{\boldsymbol{q}\nu}V_{\rm eff}$ is the change in the effective potential induced from a particular $\boldsymbol{q}\nu$ phonon mode. Precisely speaking, the electron-phonon matrix element must be corrected for the incompleteness of the basis functions, but we do not discuss it here. The expression of T_c derived by Allen-Dynes[17] by modifying the McMillan formula[18] is given as

$$T_c=\frac{\omega_{\log}}{1.2}\exp\left(-\frac{1.04(1+\lambda)}{\lambda-\mu^*(1+0.62\lambda)}\right), \tag{4}$$

where

$$\lambda=2\int_0^\infty d\omega\frac{\alpha^2F(\omega)}{\omega}, \tag{5}$$

$$\omega_{\log}=\exp\frac{1}{\lambda}\int_0^\infty\frac{d\omega}{\omega}\alpha^2F(\omega)\log\omega. \tag{6}$$

Usually λ is called the dimensionless electron-phonon coupling constant, $\omega_{\log}$ the logarithmic-averaged phonon frequency and μ^* the effective screened Coulomb repulsion constant whose value is usually taken to be between 0.1 and 0.15.

In case of monatomic metals λ can be expressed also in the following form:

$$\lambda=\frac{N(\varepsilon_F)\langle I^2\rangle}{M\langle\omega^2\rangle}=\frac{\eta}{M\langle\omega^2\rangle}, \tag{7}$$

where M is the mass of the atoms and $\langle\omega^2\rangle$ denotes the average of squared phonon frequencies which is given as

$$\langle\omega^2\rangle=\frac{\int\omega^2\dfrac{\alpha^2F(\omega)}{\omega}d\omega}{\int\dfrac{\alpha^2F(\omega)}{\omega}d\omega}. \tag{8}$$

Further $\langle I^2\rangle$ represents the Fermi surface average of squared electron-phonon coupling interaction which is defined by

$$\langle I^2\rangle=\frac{\sum_{\boldsymbol{q}\nu}\sum_{\boldsymbol{k}jj'}|g^{\boldsymbol{q}\nu}_{\boldsymbol{k}+\boldsymbol{q}j',\boldsymbol{k}j}|^2\delta(\varepsilon_{\boldsymbol{k}j}-\varepsilon_F)\delta(\varepsilon_{\boldsymbol{k}+\boldsymbol{q}j'}-\varepsilon_F)}{\sum_{\boldsymbol{q}\nu}\sum_{\boldsymbol{k}jj'}\delta(\varepsilon_{\boldsymbol{k}j}-\varepsilon_F)\delta(\varepsilon_{\boldsymbol{k}+\boldsymbol{q}j'}-\varepsilon_F)}, \tag{9}$$

and $\eta=N(\varepsilon_F)\langle I^2\rangle$ is called the Hopfield parameter.

B. Results for bcc Se

We first calculated the phonon dispersion curve along the high symmetry line (ΓN) for bcc Se at different 4 volumes (pressures), 10.37 Å^3 (214.2 GPa), 11.11 Å^3 (165.6 GPa), 11.85 Å^3 (128.6 GPa), and 12.59 Å^3 (102.59 GPa). The results are shown in Fig. 5.

As the pressure decreases, the overall tendency of decrease of phonon frequency is seen. In particular, the frequency softening is remarkable for one of the transverse modes (shown by the solid curve), and this mode exhibits a notable phonon anomaly, i.e., a dip in the middle of the line. The same phonon anomaly is obtained in *S*.[19] This softening of the transverse mode does not cause directly the bcc $\rightarrow\beta$-Po transition with decreasing pressure because both of the β-Po and bcc phases have one atom per unit cell. However Zakharov and Cohen[19] have pointed out that it plays an important role in changing the coordination number from eight to six during the bcc$\rightarrow\beta$-Po transition.

Mauri *et al.* have performed *ab initio* linear-response calculation for lattice dynamics of bcc Te under pressures.[3] They reported the same anomaly for the transverse mode

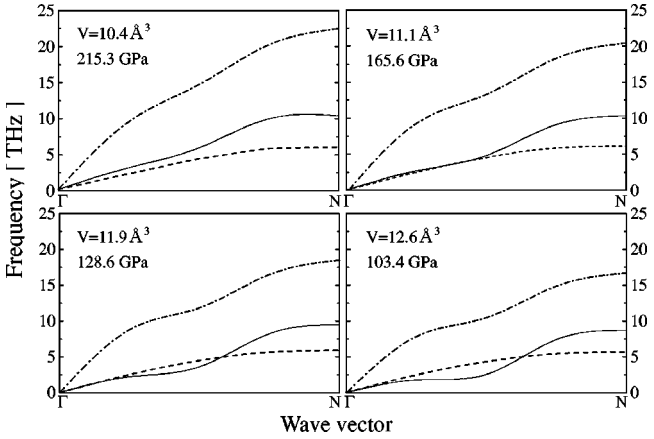

FIG. 5. The phonon dispersion along the ΓN line for bcc Se. The chain line denotes longitudinal mode, and the solid and dashed lines the transverse modes.

along the ΓN line and found that with decreasing pressure the phonon frequencies in the middle of the ΓN line become imaginary in a pressure region where the β-Po structure is stable. In our calculation complete softening of the transverse mode has not been observed even at 100 GPa where the β-Po structure is stable. Complete softening may occur at even lower pressures.

Figure 6 shows the pressure dependence of the phonon dispersion along several symmetry lines and the phonon density of state (DOS) calculated at three volumes (or pressures) 11.85 Å^3 (128.6 GPa), 11.41 Å^3 (149.6 GPa), and 11.11 Å^3 (165.6 GPa). It is noted that except along the ΓN line all the phonon frequencies soften linearly with decreasing pressure (or increasing volume).

By using the Allen-Dynes formula we have estimated the superconducting transition temperature T_c of bcc Se at three pressures: 128 GPa, 150 GPa, and 166 GPa. In Table I we give the values of calculated T_c together with DOS at the Fermi level $N(\varepsilon_F)$, the Hopfield parameter η, the logarithmic average frequency $\omega_{\log}$, the average of squared phonon frequencies $\langle\omega^2\rangle$ and the electron phonon coupling constant λ. With decreasing pressure the value of $\omega_{\log}$ decreases

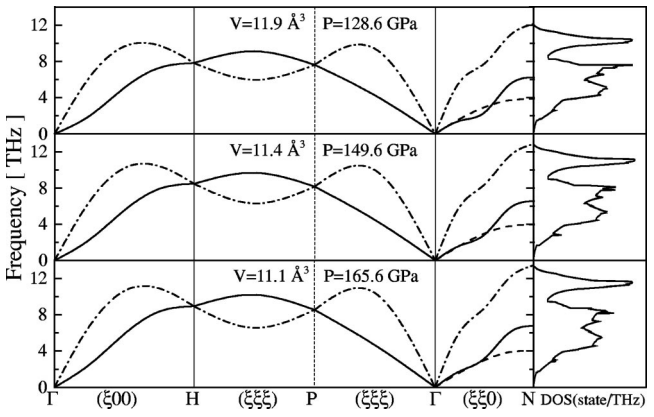

FIG. 6. The phonon dispersion and phonon density of state (DOS) for bcc Se. The chain line denotes longitudinal modes. The solid and dashed lines denote transverse modes.

TABLE I. The electronic DOS at the Fermi level $N(\varepsilon_F)$, the Hopfield parameter η, the logarithmic average frequencies $\omega_{\log}$, the average of squared phonon frequencies $\langle\omega^2\rangle$, the electron phonon coupling constant λ and the superconducting transition temperatures T_c calculated as a function of pressure for bcc Se. The two values for T_c correspond to two different values of μ^* (0.10 and 0.12). The units of $N(\varepsilon_F)$ and η are state/Ryd./atom/spin and Ryd./Å,^{2} respectively.

P (GPa)	$N(\varepsilon_F)$	η	$\omega_{\log}$ (K)	$\langle\omega^2\rangle$ (K^2)	λ	T_c (K)
128.6	2.73	0.73	224.73	291.95^2	0.83	11.29, 9.90
149.6	2.62	0.75	248.03	316.41^2	0.73	9.53, 8.11
165.6	2.55	0.77	264.62	335.11^2	0.66	8.03, 6.64

while the value of λ increases, but the rate of change of λ exceeds that of $\omega_{\log}$. As a result the value of T_c increases considerably with decreasing pressure. Since λ can be expressed by

$$\lambda = \frac{N(\varepsilon_F)\langle I^2\rangle}{M\langle\omega^2\rangle} = \frac{\eta}{M\langle\omega^2\rangle},$$

the frequency softening (decrease of $\langle\omega^2\rangle$) is considered to contribute to the increase of λ with decreasing pressure.

As for the value of μ^* we have adopted tentatively two typical values, $\mu^*=0.10$ and 0.12. Usually μ^* takes a value of 0.1∼0.15, and F. Mauri *et al.*[3] used $\mu^*=0.12$ and 0.14 in estimating T_c of bcc Te under pressures. If we use the Thomas-Fermi model for describing the screened Coulomb interaction and adopt the free electron model, the value of μ^* can be evaluated easily.[20,21] In fact, if we assume six p electrons of each Se atom behave as free electrons, we obtain $\mu^*=0.093$ at 128.6 GPa ($V=11.9$ Å^3) and 0.094 at 165.6 GPa ($V=11.1$ Å^3) for bcc Se. The value of μ^* evaluated in this way is rather insensitive to pressure, and if we use $\mu^*=0.093$ or 0.094, we obtain T_c a little bit higher than those given in Table I.

In order to obtain a more physical insight into the characteristic pressure dependence of T_c we consider mode and wave-vector dependencies of the phonon linewidths $\gamma_{q\nu}$ along the symmetry lines. Figure 7 shows that $\gamma_{q\nu}$ is almost independent of pressure except for the longitudinal mode along the ΓH line and one of the transverse modes along the ΓN.

With decreasing pressure, $\gamma_{q\nu}$ of the longitudinal mode along the ΓH decreases whereas that of the transverse mode along the ΓN line increases considerably. Generally speaking, a large phonon linewidth increases the dimensionless electron-phonon coupling λ. Therefore, it is expected that the transverse mode along the ΓN line plays an important role in giving rise to the characteristic pressure dependence of T_c.

To clarify the role of the transverse mode along the ΓN line in more detail we have calculated a quantity $\alpha^2(\omega)$ defined by

$$\alpha^2(\omega) = \frac{\alpha^2 F(\omega)}{D(\omega)}, \tag{10}$$

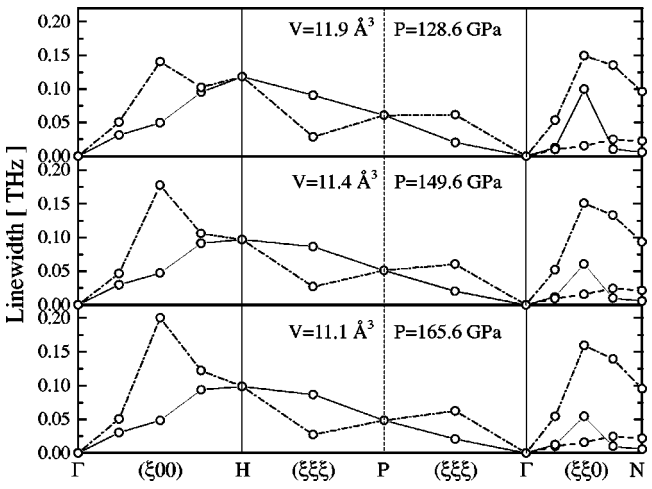

FIG. 7. The phonon line width $\gamma_{q\nu}$ calculated for three different pressures. The chain line denotes the results for the longitudinal mode, and the solid and dashed ones those for the transverse modes. Note that the transverse modes are degenerate along the (ξ00) and ($\xi\xi\xi$) lines.

where $\alpha^2F(\omega)$ is the spectral function and $D(\omega)$ denotes the phonon density of states. We consider that by inspecting the frequency dependence of $\alpha^2(\omega)$ we can discern which phonons make dominant contributions to the dimensionless electron-phonon coupling λ. Figure 8 shows the calculated $\alpha^2(\omega)$ as a function of frequency for three pressures. The peak around 2 THz originates from transverse phonons along the ΓN line and the peak around 7~10 THz from longitudinal phonons along the ΓH line. As seen from the figure, both the peaks move towards the lower frequency side with decreasing pressure. It should be noted, however, that the magnitude of $\alpha^2(\omega)$ around 2 THz increases remarkably with decreasing pressure whereas the magnitude of $\alpha^2(\omega)$ around 7~10 THz is less dependent on pressure. Therefore, we can say again that transverse phonons in the middle of the ΓN line make a dominant contribution to λ.

Combining all of the above results we conclude that the origin of remarkable increase of T_c of bcc Se with decreasing pressure is mainly attributed to the phonon anomaly (the remarkable frequency softening) in the middle of the ΓN line.

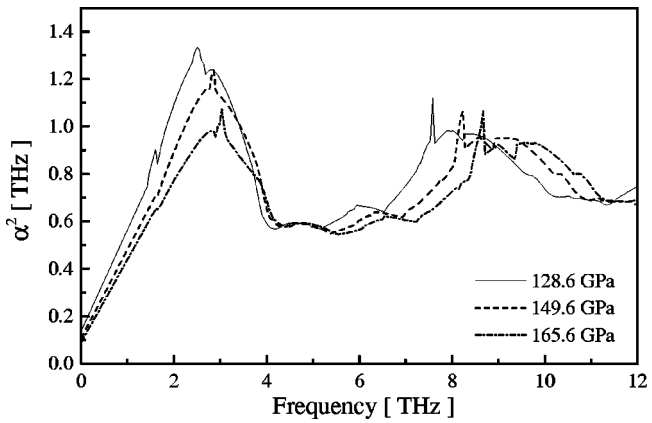

FIG. 8. The frequency dependence of $\alpha(\omega)^2$ obtained for three pressures.

TABLE II. Two sets of lattice constants c/a and a of β-Po Se determined by calculation and experiments.

[GPa]	103.1 calc.	103.1 Exp.	118.2 calc.	118.2 Exp.
c/a	0.71	0.75	0.67	0.74
a (Å)	3.95	3.87	3.97	3.84

C. Results for β-Po Se

In this section we calculate the superconducting transition temperature of β-Po Se. To see the pressure dependence of T_c in β-Po Se we have calculated T_c at pressures 103.1 GPa and 118.2 GPa with two sets of lattice constants: one is the lattice constants evaluated by calculation and the other is those determined by experiment and given in Table II. Figure 9 shows the electronic dispersion curves and the density of states calculated for 103.1 GPa.

The calculated T_c are given in Table III together with the electronic DOS at the Fermi level $N(\varepsilon_F)$, the Hopfield parameter η, the logarithmic average frequency ω_{log}, the average of squared phonon frequencies $\langle\omega^2\rangle$ and the electron phonon coupling constants λ. T_c strongly depends on which sets of lattice constants is used. For the lattice constants estimated by calculation, the magnitude of T_c is larger and increases considerably with decreasing pressure. For lattice constants determined by measurements, on the other hand, the magnitude of T_c is smaller and depends little on pressure.

The logarithmic average frequencies ω_{log} are larger for the experimental lattice constants. The electron-phonon coupling λ, on the other hand, is larger for the theoretical lattice constants and furthermore depends considerably on pressure, which gives higher and more pressure-sensitive transition temperatures T_c for the theoretical lattice constants.

In order to clarify the origin of the different magnitude and the different pressure dependence of T_c for different sets

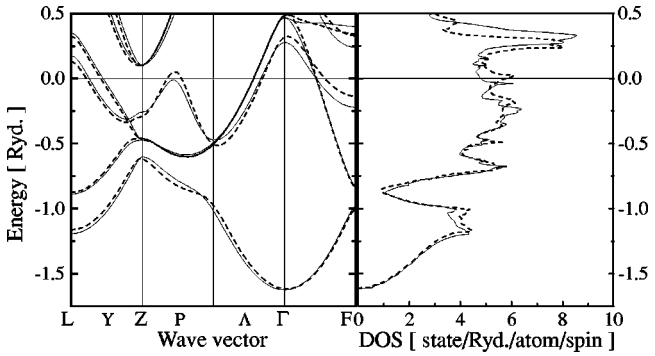

FIG. 9. The band structure and the DOS of β-Po Se at atomic volume $V=12.59$ Å (103.1 GPa). The dashed curves denote the results obtained with use of lattice constants estimated by calculation and the solid ones those with use of lattice constants determined by experiments (Ref. 13). The horizontal line denotes the Fermi level.

TABLE III. The electronic DOS at the Fermi level $N(\varepsilon_F)$, the Hopfield parameter η, the logarithmic average frequencies $\omega_{\log}$, the average of squared phonon frequencies $\langle\omega^2\rangle$, the electron phonon coupling constant λ, and the superconducting transition temperatures T_c of β-Po Se calculated for 103.1 GPa and 118.2 GPa. The upper two lines show the results obtained with use of the lattice constants estimated by calculation and the lower two lines those with use of the lattice constants determined by experiments. The two values for T_c correspond to two different values of μ^* (0.10 and 0.12). The units of $N(\varepsilon_F)$ and η are state/Ryd./atom/spin and Ryd./Å,^{2} respectively.

P (GPa.)	$N(\varepsilon_F)$	η	$\omega_{\log}$ (K)	$\langle\omega^2\rangle$ (K^2)	λ	T_c (K)
103.1	2.62	0.66	192.98	264.72^2	0.92	11.74, 10.49
118.2	2.75	0.66	204.84	279.76^2	0.82	10.10, 8.84
103.1	2.45	0.58	250.11	311.71^2	0.58	5.14, 4.04
118.2	2.43	0.62	255.88	324.58^2	0.57	5.01, 3.91

of lattice constants we have calculated the phonon density of states $D(\omega)$, the spectral function $\alpha^2F(\omega)$ and $\alpha^2(\omega)$ defined by Eq. (10). The results are shown in Fig. 10. The magnitude of $\alpha^2(\omega)$ for the theoretical lattice constants is larger than that for the experimental lattice constants throughout almost the whole frequency range. In particular the magnitude of a peak in $\alpha^2(\omega)$ around 2 THz obtained for the calculational lattice constants is remarkably enhanced compared to that obtained for the experimental ones, thus the magnitude of λ and T_c take large values. For the experimental lattice constants, $\alpha^2(\omega)$ depends little on pressure and hence the magnitude of λ and T_c are also less dependent on pressure.

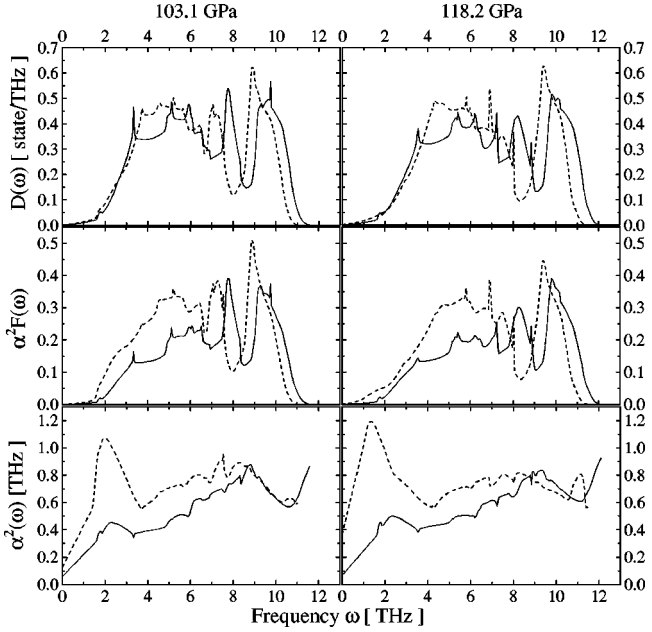

FIG. 10. The phonon density of states $D(\omega)$, the spectral function $\alpha^2F(\omega)$, and $\alpha^2(\omega)$ defined by Eq. (10) calculated for pressures 103.1 GPa (left-hand side) and 118.2 GPa (right-hand side) with use of the theoretical and experimental lattice constants. The dashed curves represent the results for the theoretical lattice constants and the solid curves for the experimental lattice constants.

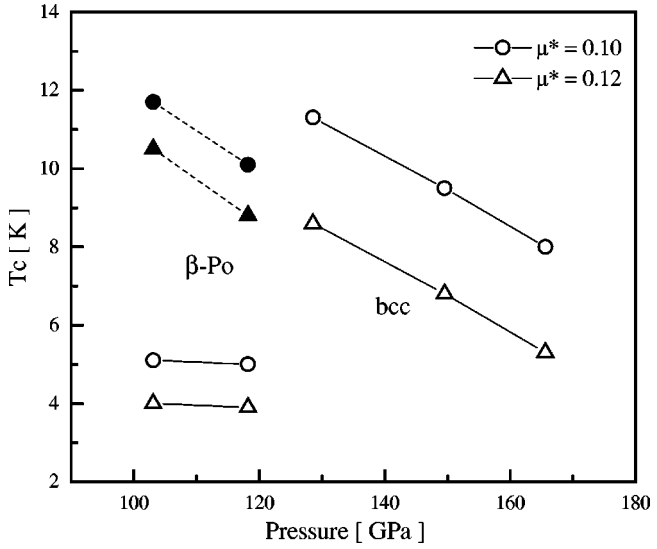

FIG. 11. The circles and triangles denote the computed values of T_c with $\mu^*=0.10$ and $\mu^*=0.12$, respectively. For the β-Po structure the closed circles and triangles represent the results for the lattice constants estimated by calculation and the open circles and triangles those for the lattice constants determined by experiments.

Figure 11 shows the values of T_c calculated for β-Po and bcc Se as a function of pressure. If we adopt the experimental lattice constants for β-Po Se, the superconducting transition temperature T_c is almost pressure independent in the β-Po phase and there is a large jump in T_c at the transition from β-Po to bcc.

IV. CONCLUSION

We have performed the FPLMTO calculation for the β-Po and the bcc structures of selenium, and succeeded in reproducing the phase transition from β-Po to bcc as observed by experiments. The obtained pressure dependencies of lattice parameters agree fairly well with the experimental results. The estimated transition pressure is 120 GPa. It improves the previous theoretical calculations, but is still lower than the experimental value 150 GPa.

We have investigated the superconductivity of β-Po and bcc Se by calculating the lattice dynamics and electron-phonon interaction with use of LR-FPLMTO method. For bcc Se we have found that the frequency softening is remarkable for one of the transverse modes in the middle of the ΓN line, and this mode exhibits a notable phonon anomaly. The calculated superconducting transition temperature T_c increases considerably with decreasing pressure, which is mainly attributed to the phonon anomaly in the middle of the ΓN line. In the β-Po structure, the calculated values of T_c depends sensitively on the lattice constants we have used. For the lattice constants estimated by calculation, the values of T_c is as high as that in bcc phase and decreases rapidly with increasing pressure. If we use the lattice constants determined by measurements, on the other hand, T_c is almost pressure independent and there is a large jump in T_c at the transition from β-Po to bcc.

ACKNOWLEDGMENTS

We thank greatly Dr. S.Yu. Savrazov of Max Planck Institute for providing us with the FPLMTO and LR-FPLMTO program. We are grateful to Professor Y. Akahama for showing us their experimental results prior to publications. One of the author (M.O.) thanks Professor M. Shirai for illuminating and valuable discussion about linear-response theory and also Dr. K. Yamaguchi for fruitful discussion about FPLMTO method. This work is partly supported by Grant-in-Aid for COE Research (No. 10CE2004) and Grant-in-Aid for Scientific Research (C) (No. 09640433) of the Ministry of Education, Science, Sports and Culture. M.O. is supported by the JSPS Research Fellowships for Young Scientists.

*Present Address: Institute for Solid State Physics, The University of Tokyo, Kashiwa, Chiba 277–8581, Japan.

[1] G. Parthasarathy and W. B. Holzapfel, Phys. Rev. B **37**, 8499 (1988).
[2] Y. Akahama, M. Kobayashi, and H. Kawamura, Solid State Commun. **84**, 803 (1992).
[3] F. Mauri, O. Zakhalov, S. de Gironcoli, S.G. Louie, and M.L. Cohen, Phys. Rev. Lett. **77**, 1151 (1996).
[4] S.Yu. Savrasov and D.Yu. Savrasov, Phys. Rev. B **46**, 12 181 (1992).
[5] S.Yu. Savrasov, Phys. Rev. B **54**, 16 470 (1996).
[6] S.Yu. Savrasov and D. Yu Savrasov, Phys. Rev. B **54**, 16 487 (1996).
[7] S.Yu. Savrasov and O.K. Anderson, Phys. Rev. Lett. **77**, 4430 (1996).
[8] V. Meregalli, S.Yu. Savrasov, Phys. Rev. B **57**, 14 453 (1998).
[9] O. Gunnarsson and B.I. Lundqvist, Phys. Rev. B **13**, 4274 (1976).
[10] J.P. Perdew, K. Burke, and Yu. Wang, Phys. Rev. B **54**, 16 533 (1996).
[11] P.E. Blöchel, O. Jepsen, and O.K. Andersen, Phys. Rev. B **49**, 16 223 (1994).
[12] F.D. Murnaghan, Proc. Natl. Acad. Sci. U.S.A. **30**, 244 (1944).
[13] Y. Akahama, M. Kobayashi, and H. Kawamura, Phys. Rev. B **47**, 20 (1993).
[14] M. Geshi, T. Oda, and Y. Hiwatari, J. Phys. Soc. Jpn. **67**, 3141 (1998).
[15] A. Nishikawa, K. Niizeki, and K. Shindo, Jpn. J. Appl. Phys. **32**, Suppl. 32-1 48 (1993).
[16] G.M. Eliashberg, Zh. Éksp. Teor. Fiz. **38**, 966 (1960) [Sov. Phys. JETP **11**, 696 (1960)].
[17] P.B. Allen and R.C. Dynes, Phys. Rev. B **12**, 905 (1975).
[18] W.L. McMillan, Phys. Rev. B **12**, 331 (1968).
[19] O. Zakharov and M.L. Cohen, Phys. Rev. B **52**, 12 572 (1995).
[20] P. Morel and P.W. Anderson, Phys. Rev. **125**, 1263 (1962).
[21] H. Sakamoto, T. Oda, M. Shirai, and N. Suzuki, J. Phys. Soc. Jpn. **65**, 489 (1996).